BMP2 and BMP7 play antagonistic roles in feather induction

Michon Frédéric [1] , Forest Loïc [2] , Collomb Elodie [1] , Demongeot Jacques [2] , Dhouailly Danielle [1 *]

[1] Institut d'oncologie/développement Albert Bonniot de Grenoble INSERM : U823, CHU Grenoble, EFS, Université Joseph Fourier - Grenoble I, Institut Albert Bonniot, BP170, 38042 Grenoble Cedex 9,FR

[2] TIMC, Techniques de l'Ingénierie Médicale et de la Complexité CNRS : UMR5525, Université Joseph Fourier - Grenoble I, Domaine de la Merci 38710 La Tronche,FR

* Correspondence should be adressed to: Danielle Dhouailly <danielle.dhouailly@ujf-grenoble.fr>

Abstract
Summary

During embryonic development, feathers first appear as primordia consisting of an epidermal placode associated with a dermal condensation. In most previous studies, the BMPs have been proposed to function as inhibitors of the formation of cutaneous appendages. We showed that the function of BMPs is quite nuanced: BMP-2 and BMP-7, which are expressed in both skin components, act antagonistically and yet are both involved in the dermal condensations formation. BMP-7, the first to be expressed, is implicated in chemotaxis which leads to cell recruitment to the condensation, whereas BMP-2, which is expressed later, leads to an arrest of cell migration, likely via its modulation of EIIIA Fibronectin domain and 4-Integrin expression. We also propose a mathematical model, a reaction-diffusion system, based on cell proliferation, chemotaxis and the timing of BMP-2 and BMP-7 expression, which simulates the endogenous situation and reproduces the negative effects of excess BMP-2 or BMP-7 on feather patterning.

Author Keywords dermis ; cutaneous appendage ; chemotaxis ; migration ; Fibronectin ; mathematical model ; skin

Introduction

The chick skin can be divided into different domains: pterylae (feather area), semi-apteria (with a few feathers) and apteria (glabrous area) (Mayerson and Fallen, 1985; Sengel, 1976). The future pterylae are characterized by the formation of dense dermis (Sengel, 1976). In the dorsal pterylae, this occurs from days 5 to 6.5 of incubation (stages HH25 to HH29 (Hamburger and Hamilton, 1951)), and at day 7 (HH30) the midline, where the first row of feathers will appear, undergoes a further density increase. Before cell migration occurs, leading to dermal condensation, cells proliferate until a threshold is reached (2.60 nuclei/1000µm^3 (Desbiens et al., 1991; Jiang and Chuong, 1992; Wessells, 1965)). In contrast, in semi-apteria the cell density remains under this threshold: 2.0 nuclei/1000µm^3 (Olivera-Martinez et al., 2001). When cell density exceeds the threshold, proliferation stops and there is redistribution (Michon et al., 2007) of cells to form dermal condensations (5.52 nuclei/1000µm^3, (Wessells, 1965)) under placodes. These two structures form the feather primordium. The lateral propagation of this process creates a hexagonal feather pattern.

Numerous pathway (Chuong, 1998) have been implicated in the cross-talk between the epidermis and the dense dermis (Dhouailly, 1977) leading to feather morphogenesis. The exact regulation of the cross-talk, in the narrow time window available for primordium formation is not clear. The different signals involved in feather primordium formation are classified as activators and as inhibitors (Jung et al., 1998). The FGF pathway, an activator pathway, is implicated in both epidermal and dermal differentiation (Tao et al., 2002; Widelitz et al., 1996). Epidermal FGF-2 expression is involved in dermal condensation formation via its chemotaxic effect on fibroblasts (Song et al., 1996; Song et al., 2004; Viallet et al., 1998). Of the BMP family, inhibitor of feather formation, three members are expressed in the feather primordium domain: BMP-2, BMP-4 and BMP-7, where BMP-2 and -4 belong to the same subgroup (Miyazono et al., 2005). BMP-2 is initially expressed in the epidermis, and later restricted to the placode and dermal condensation (Noramly and Morgan, 1998). BMP-4 transcripts are detected only in the forming dermal condensation (Noramly and Morgan, 1998). BMP-7 is expressed throughout the epidermis before placode formation and is subsequently restricted to the primordium, in both dermis and epidermis (Harris et al, 2004). BMP-2 expression comes on earlier than BMP-4 (Houghton et al., 2005), and later than BMP-7 (Harris et al., 2004). The transcriptional regulation of BMP-2 and BMP-4 expression in embryonic skin is still unknown. BMP-7 is expressed in the epidermis under the control of an unknown dermal signal, whereas its dermal expression is regulated by the canonical Wnt pathway from the placode (Harris et al., 2004).

The BMP pathway is currently considered as an inhibitor of feather (Jung et al., 1998), as well as hair (Botchkarev, 2003), or tooth formation (Pummila et al., 2007). The application of BMP-4 coated beads on explanted chick HH28 (E6) dorsal skin inhibits adjacent feather bud formation (Jung et al., 1998). In addition, over-expression of BMP-4 in the chick embryo dorsal skin, via infection with RCAS virus, leads to the formation of glabrous areas (Noramly and Morgan, 1998). However, the different studies addressing the role of BMPs in feather

formation are contradictory. The application of BMP-7 coated beads inhibits feather formation (Patel et al., 1999), whereas its expression has been shown to be required (Harris et al., 2004). Likewise, an ectopic feather forming dermis can be obtained in two opposite ways: by the inhibition of BMP pathway in the mid-ventral apterium (Fliniaux et al., 2004), or by a BMP-4 coated bead in the dorso-scapular semi-apterium (Scaal et al., 2002). These apparently contradictory results might be explained by spatial factors, as the molecular mechanisms responsible for the establishment of the dermis in the back and the ventral region are different (Fliniaux et al., 2004; Olivera-Martinez et al., 2002). With respect to the contradictory results for the back region, it is interesting to note that different concentrations of BMP are used. The use of RCAS infection (Noramly and Morgan, 1998) or high concentration coated beads (660µg/ml) leads to an inhibitory effect (Jung et al., 1998), while the use of low concentration coated beads (20µg/ml) (Scaal et al, 2002) leads to activation. Other results also appear to contradict the proposed inhibitor role of BMP signaling. Msx-1 and Msx-2, two BMP target genes, are expressed in the placode (Noveen et al., 1995). Two principal BMP signaling antagonists have been identified in chick skin, Follistatin and Drm/Gremlin. Although Follistatin expression, regulated by BMP-7, initially occurs throughout the follicular domain, it shifts rapidly to a peripheral ring when the placode is formed (Patel et al., 1999), while Drm/Gremlin is restricted to the interfollicular domain (Bardot et al., 2004). A recent study has proposed the Eda/Edar pathway as BMP antagonist for hair formation (Pummila et al., 2007), but in chick these molecules are expressed after BMP-2 (Houghton et al., 2005). Altogether, the expression of BMP target genes and the absence, or the transient expression, of BMP inhibitors in the follicular domain, as well as the importance of the BMP amount delivered experimentally, indicate a more nuanced role for the BMPs.

In order to investigate the nuances of the role of BMP signaling in embryonic skin we examined three different aspects of BMP signaling and dermal condensation formation in chick. Firstly, we investigated in vivo the expression of another set of downstream targets of BMP signaling, the Id genes (Hollnagel et al., 1999), known to modify cell differentiation (Kreider et al., 1992; Miyazono and Miyazawa, 2002; Ogata et al., 1993). In chick, four Id genes have been reported (Kee and Bronner-Fraser, 2001), and we studied their expression in skin. Secondly, we addressed in vitro the issue of dermal fibroblast behavior. For the transition from a dense dermis to the dermal condensation, fibroblast migration (Mauger et al., 1982) and Fibronectin have been implicated (Chuong, 1993; Michon et al., 2007). Alternative splicing of Fibronectin has been identified as a key regulator of Integrin affinity in CHO cells, with the EIIIA domain modulating the Fibronectin/Integrin interaction (Manabe et al., 1997). Another role of the EIIIA domain is its ability to induce the G1-S transition by promoting adhesion on α5β1 Integrin (Manabe et al., 1999). We thus studied the changes in the EIIIA domain expression during dermal organization. Thirdly, we established in silico a mathematical model based on an activation/inhibition diffusion Turing system (Turing, 1952), that takes into account the new parameters of cell density and migration. Our numerical simulation was in agreement not only with our current biological experimental results, but also explained previous apparently contradictory results (Jung et al, 1998; Noramly and Morgan, 1998).

We showed that instead of acting as inhibitors of feather formation, BMPs play several roles, from the regulation of dermal condensation formation to the continuation of feather morphogenesis.

Materials and methods

Materials

Fertilized eggs (JA957 strain, St Marcellin, France) were incubated seven days at 38°C until the embryos reached Hamburger Hamilton stage 29 or 30 (Hamburger and Hamilton, 1951). rhBMP-2, rhBMP-7 and rhFGF-2 were purchased from R&D Systems Europe.

Organotypic skin in vitro culture

Seven-day chick embryo (stage HH29 or 30) dorsal skins were dissected as a single piece starting from the wing to the femoral level. They were cultured as previously described (Michon et al, 2007). For local application, 150 to 200µm diameter Affi-gel Blue beads (Bio-Rad) were soaked into PBS or rhBMP-7 (concentrations specified in figure legends) and then placed on the explants.

Dermal fibroblast in vitro culture

The dermis was separated from the epidermis after Trypsin 1.25%/Pancreatin 4% (Sigma-Aldrich) treatment, then mechanically dissociated into a single cell suspension. Cells were used for RT-PCR, adherent cell culture, cell migration assay or micromass formation. To evaluate the cell migration, 25.10^4 cells were used for each condition in the Innocyte cell migration assay (VWR International) (Lauffenburger, 1996). The migration was measured after 10 hours by Calcein-AM dye. Fetal Bovine Serum was used as an attracting factor for cells as a positive control. The micromass culture was performed as previously described (Michon et al., 2007).

FACS analysis

HH29 and HH30 chick embryo dorsal skins were dissected in medial and lateral parts separated of lateral ones. Obtained dermal cell suspensions were fixed in cold ethanol (2.10^6 cells/ml). Cell aggregates were broken mechanically and cells were labeled in 0,1% NP40,

0,1mg/ml RNAse A, 50µg/ml Propidium Iodide (Sigma). Cells were rinsed in PBS and analysis performed with CellQuest Pro software (Becton Dickinson).

Molecular Biology

RNA was isolated with the High Pure RNA tissue kit (Roche). Reverse transcription was performed with the Superscript First-Strand synthesis system (Invitrogen). PCR products were analyzed with the ImageJ software (NIH). Primers used: cActin sense: AGACCTTCAACACCCCAGC; cActin antisense: TGATTTTCATTGTGCTAGG; cEIIIA sense: ATGGTACAGCGTCTATGCTCA; cEIIIA antisense: AGACTGGTAGGAGTTACCTGA; Fibronectin sense: CAGTGGCTACCGAGTGACCAC; Fibronectin antisense: AGACTGGTAGGAGTTACCTGA. Primers for chick Actin were designed to discriminate between genomic and complementary DNA (926pb vs 619pb).

In situ hybridization

The chick EIIIA probe was cloned into the pGEM-T Easy vectors (Promega, France) (based on its published sequence, (Norton and Hynes, 1987)). The cBMP-2 and cBMP-7 probes were a gift from Dr. A-H. Monsoro-Burq. The cFollistatin probe was a gift from Dr. A. Graham. The cId-1, cId-3, cId-4 and cα4Integrin probes were a gift from Dr. M. Bronner-Fraser. Alkaline phosphatase-labelled in situ hybridizations were carried out as previously described (Wilkinson and Nieto, 1993).

Results

The BMP pathway appears implicated in early feather primordium formation

As the two femoral feather tracts of the same embryo develop synchronously on the left and right sides, it is possible to compare gene expression timing (Houghton et al, 2005). Feather rows were numbered accordingly to the order of appearance. The femoral tract has seventeen rows, fifteen proximal to the first one. Distal to the first row, a discontinuous line of expression which gives rise to the third row occurred. This third row forms the boundary between femoral and zeugopodial tracts, which are on each side of a semi-apteria. The expressions of BMP-2 and BMP-7 in the corresponding feather primordia of the left and right halves of the same embryo were compared at HH30 (n=6/6 for each comparison). In the second row of this tract, BMP-2 was expressed in only two feather primordia (Fig. 1A), instead of in five primordia for BMP-7 (Fig. 1B). Follistatin (Fig. 1D), a BMP inhibitor, was expressed after BMP-2 (Fig. 1C). The BMP target genes Ids, Id-1, Id-3 and Id-4 transcripts were detected in HH30 chick embryo dorsal skin in the primordium (Fig. 1E–G). Id-4 expression appeared initially in the complete primordium (newly formed rows), but subsequently the transcripts were detected only as a peripheral ring (Fig. 1G). The expressions of Id-1 and Id-4 were concomitant to that of BMP-2 (Fig. S1A–D), and the expression of Id-3 to that of BMP-7 (Fig. S1E–F). All taking together, the BMP pathway appeared to be involved in feather primordium formation.

BMP-2 and BMP-7 have opposite effects on dermal fibroblast migration

In order to distinguish the role of BMP-2 and BMP-7, we quantified their effects on migration through a membrane under various conditions (Fig. 2). Two kinds of controls were performed. First, we used the basic medium with or without 10% Fetal Bovine Serum (FBS) which has a known chemoattractive effect. Secondly, we added FGF-2 to the basic media, which is known to have a positive chemoattractive effect on dermal cells (Song et al., 2004). Each result, done in triplicate, was measured relative to the cell migration obtained with the basic medium containing FBS (100%). Without FBS, cell migration decreased to 50.1% ($p<0.001$). FGF-2 activated cell motility, both in presence (+11.9%, $p<0.01$) or absence (+10.7%, $p<0.01$) of FBS. Interestingly, BMP-7 had an even stronger effect than FGF-2 at +22.2% ($p<0.01$) in the presence or +20% ($p<0.01$) in the absence of FBS, while BMP-2 had an inhibitory effect on migration: −18.7% ($p<0.01$) with and −11.9% ($p<0.01$) without FBS. Combining BMP-2 and BMP-7 in the same medium cancelled out the effect of each factor on dermal cell migration: the difference between the chemotactic effect of both BMPs or only BMP-7 was striking: −24.1% ($p<0.02$) with and −18.9% ($p<0.01$) without FBS. Our in vitro assay was independent of extracellular matrix, but in vivo, there might be interactions between the BMPs and the extracellular matrix.

BMP-2 modifies the EIIIA Fibronectin domain and 4-Integrin expressions

Analysis of the EIIIA Fibronectin domain in chick embryo dorsal skin showed a lack of expression in fully-formed dermal condensations at HH29+, whereas its expression was high in areas where the dense dermis was still undergoing organization (Fig. 3A). At HH30, there was a lateral expansion of EIIIA domain expression and a slight decrease of expression in the interfollicular domain of the first rows formed (Fig. 3B). To analyze the timing of the loss of the EIIIA domain expression, we compared the timing of its expression with BMP-2 (n=9/9). Whereas

BMP-2 was expressed in five primordia on the fourth row (Fig. 3C), the loss of EIIIA expression occurred only in two primordia of the same row (Fig. 3D). Furthermore, a strong expression was detected at the distal boundary of the tract close to the third row which has started to form. The expression of BMP-2 thus preceded the alternative splicing of the EIIIA Fibronectin domain.

To study the alternative splicing of EIIIA, we have used freshly isolated dermal cells in two complementary methods. In order to mimic the formation of dermal condensations in vitro by dispersed fibroblasts, we used the micromass method (Michon et al, 2007) to follow cell aggregation for 3 days. Semi-quantitative RT-PCR (n=3) were performed in order to follow Fibronectin and EIIIA expressions (Fig. 4). There was a slight decrease of Fibronectin expression from t_0 (100%) to t_{72} (64.1%) (Fig. 4A), but the proportion of Fibronectin containing the EIIIA exon has drastically decreased, from 59.4 to 24.3% during the same time (Fig. 4B). The relative decrease of EIIIA domain expression was also induced in adherent cell culture via the addition of BMP-2. Semi-quantitative RT-PCR of primary cultured dermal fibroblast showed expression of the EIIIA domain after 20 hours of culture under control conditions, whereas the addition of BMP-2 led to a decrease of the part of Fibronectin containing EIIIA after 20 hours of treatment, from 61.1% to 34.4% (Fig. 4C). There was a slight effect due to BMP-7 treatment, from 61.1% to 53.1%.

α4-Integrin was expressed in the follicular domain (data not shown) as it was previously shown in the dental mesenchyme condensation (Jaspers et al., 1995). The addition of BMP-2 induced the over-expression of α4-Integrin as well, from 100% to 125.3% (Fig. 4D), the addition of BMP-7 led to a non significant increase of α4-Integrin expression, from 100% to 105.54%. As the EIIIA domain was not only shown to modulate Fibronectin/Integrin interaction, but also to be implicated in the control of cell proliferation (Manabe et al., 1999), we wanted to quantify the population of cycling cells in the dorsal skin before and after dermal condensation formation.

Cell proliferation in the chick embryo dorsal skin at HH29 and HH30

Cycling cells have been previously localized in the interfollicular dermis and not in the formed dermal condensation (Rouzankina et al., 2004; Wessells, 1965). We studied cell proliferation during dermal condensation formation in chick embryo dorsal skin from HH29 to HH30. At these stages, the dorsal skin can be divided into three parts: the medial part, carrying the first dermal condensation at HH30, and two lateral parts, surrounding this (Fig. S2A–B). The proportion of cycling dermal cells in each part was determined via flow cytometry (Fig. S2C). At HH29, the difference between the lateral and medial parts was not significant: 83.7% of cells in G1 in the medial part, compared to 78.9% in the lateral part. The slight decrease of cycling cells in the medial part might reflect the start of dermal condensation formation. At HH30, the central part of the dermis (where dermal condensations are forming) had 90.9% of cells in G1, whereas in the lateral part only 77.5% of dermal cells were in G1. The proliferation of dermal cells just before condensation formation is likely to be an important factor leading to the establishment of the required cell density.

Mathematical model for dermal condensation formation and patterning

Our results allowed us to build a new mathematical model for feather primordia formation which included cell proliferation and cell migration, regulated by BMP-7 and BMP-2 expressions. The model for BMPs dynamics was inspired by activator-inhibitor model proposed by Gierer and Meinhardt (Gierer and Meinhardt, 1972). Cell migration is given by a chemotactic term as in previous studies (Cruywagen et al, 1992; Painter et al, 1999). BMP-7 is an activator of feather primordium formation via its effect on chemotaxis and cell recruitment, whereas BMP-2 counteracts the positive effect of BMP-7 on cell migration. Another important issue is that the model can be run from initial conditions consistent with the in vivo situation in the chick embryo dorsal skin at HH29.

The mathematical model described the spatiotemporal dynamics of four variables: n_1 n_2, u and v in a two dimensional space Ω. The dermal cell population, which concentration is noted n ($n = n_1 + n_2$), was divided into two subpopulations n_1 (cycling cells), and n_2 (migrant cells), u and v represent the concentration and cellular effect of BMP-7 and BMP-2.

Cellular dynamics

n_1 cells proliferation is modeled by a logistic growth function where k_p is the proliferation constant and N the maximal cell population. n_1 proliferated until they reached a threshold of cell density n^* at the time t^*. After the concentration overcame the threshold, n_1 cells progressively stopped proliferating and became able to migrate. This transition is determined by a “differentiation” constant k_d . For n_2 cells, the migration flux was modeled by a diffusive part with constant D_n and a chemotactic part with a constant χ. The chemoattractant is u.

Equations for n_1 and n_2 are:

$$\frac{\partial n_1}{\partial t} = \begin{cases} k_p n_1 (N - n_1) & \text{if } t \le t^* \\ -k_d n_1 & \text{else} \end{cases}$$

$$\frac{\partial n_2}{\partial t} = D_n \Delta n_2 - \nabla \cdot (\chi n_2 \nabla u) + \begin{cases} 0 & \text{if } t \le t^* \\ k_d n_1 & \text{else} \end{cases}$$

$n_{1,0}$, and $n_{2,0}$ are the initial conditions for n_1 and n_2 . No flux boundary condition is used for n_2 .

BMPs dynamics

u and v dynamics have been given by reaction-diffusion equations. D_u and D_v denoted the respective diffusion constants. Reaction terms were made of a linear degradation part (with constants k_u and k_v) and a production part. The production part for each chemical was constructed so as to respect the qualitative regulation between them. As they are synthesized by n_2 cells, production terms are also taken proportional to n_2 . We have:

$$\frac{\partial u}{\partial t} = D_u \Delta u + \frac{c_1 n_2 (1 + c_2 u^2)}{(c_3 + u^2)(1 + v)} - k_u u$$

$$\frac{\partial v}{\partial t} = D_v \Delta v + c_4 n_2 u^2 - k_v v$$

c_1, c_2, c_3 and c_4 are positive constants.

Production terms stated that BMP-7 expression was reinforced by “spot” (dermal condensation) microenvironment. Its chemotactic effect was inhibited by BMP-2. And both BMP-2 and BMP-7 were expressed by the same cell population (primordium domain). Initial conditions for u and v are given by u_0 and v_0 generally taken equal to 0. No flux boundary conditions are used for u and v.

Resulting model

The simple dynamics for n_1 cells allows the exact computation of n_1 (x, y, t). If n* is defined as a fraction Q of the maximal cell density N, n* = QN, we have: $n_1(x, y, t) = \frac{N n_{1,0}(x, y) e^{N k_d t}}{N + n_{1,0}(x, y)(e^{N k_d t} - 1)}$ for $t \le t^*(x, y)$ and then $n_1(x, y, t) = n^* e^{k_d (t^* - t)}$. $t^*(x, y)$ is given by: $t^*(x, y) = \frac{1}{N k_d} \ln \left(\frac{Q(N - n_{1,0}(x, y))}{n_{1,0}(x, y)(1 - Q)} \right)$. This allows directly expressing the production term of n_2 cells as a delayed production term and reducing the model as follow:

$$\begin{cases} \frac{\partial n_2}{\partial t} = D_n \Delta n_2 - \nabla \cdot (\chi n_2 \nabla u) + \begin{cases} 0 & \text{if } t \le t^* \\ k_d n^* e^{k_d (t^* - t)} & \text{else} \end{cases} \\ \frac{\partial u}{\partial t} = D_u \Delta u + \frac{c_1 n_2 (1 + c_2 u^2)}{(c_3 + u^2)(1 + v)} - k_u u \\ \frac{\partial v}{\partial t} = D_v \Delta v + c_4 n_2 u^2 - k_v v \end{cases}$$

Numerical simulations

The calculations were made using the software COMSOL Multiphysics 3.2 © and the finite element method using squared meshes. We took $\Omega =]-1,1[\times]0, 1[$ and the parameters in Table S1.

For the sequential spots appearance numerical experiment the initial situations for n_1 and n_2 are given by: $n_{1,0}(x) = 0.25 + 1.7\exp(-5x^2) + 0.2\exp(-200x^2)$ and $n_{2,0}(x) = 0.05 + 2\exp(-200x^2)$. All other initial values are set to 0. Pulse experiments are realized using the same initial

situation. Pulses are modeled by additional production terms in the equation of the BMP-7 or BMP-2. For the local pulse of BMP-7 experiment, equation (3) becomes equation (3)′: $\frac{\partial u}{\partial t} = D_u \Delta u + \frac{c_1 n_2 (1 + c_2 u^2)}{(c_3 + u^2)(1 + v)} - k_u u + p_u$ where p_u (x, y) = 25exp(−500(x ^{2}+(y−0.5)^2)). This expression of the additional term allows specifying a sharp pulse located in the centre of the domain. For the global pulse of BMP-2 we used the new term: p_v = 1000 and equation (4) becomes equation (4)′: $\frac{\partial v}{\partial t} = D_v \Delta v + c_4 n_2 u^2 - k_v v + p_v$.

To investigate the impact of cell density on the pattern, we run the model from initial situations where n_2 cells are homogenously distributed in the domain with a density q, affected by small random fluctuations. n_1 cells are not modeled. Patterns are observed at the same time t=1000.

Dermal condensation formation obtained with numerical resolution

The result of running the simulation was the formation of a pattern of spots that closely resembles the in vivo feather pattern: a medial first row followed by the lateral formation of new rows leading to a hexagonal pattern (Fig. 5A–D; Movies S1 and S2). Based on previous observations of our laboratory (Olivera-Martinez et al, 2001), we included the cell densities in the dermis of apterium, semi-apterium and pteryla before and during the primordium formation in the model parameters. For the formation of a hexagonal pattern, the cell density threshold (N=2.6) and its repartition between primordium (n=5.5) and interfollicular (n=1.5) was in accordance with the in vivo observations. For the feather tract formation, a cell density threshold (q=1) was required (Fig. 6A). Under this threshold (q=0.2 to 0.12), the pattern formation was not regular (Fig. 6B and C), similar to what is observed in semi-apteria. The cell density limit was obtained with q=0.11 where no spots were formed (Fig. 6D), similar to what occurs in vivo in the apteria.

The increase of activator led to an inhibition with our model and in vitro

Using our mathematical model, an increase of the local pulse concentration of activator led to the increase of cell recruitment under the source according to the chemotactic effect. The excess of cell recruitment resulted in an area of lower cell density around the source that could not support the formation of spots. The inhibition of spot formation followed the over-activation of cell recruitment but the pattern was maintained beyond this circle of depleted cell density (Fig. 7A–C; Movies S3, S4). These results have been also obtained in vitro (Fig. 7D–F). The diameter of the circle lacking formation of dermal condensations has increased with the application of BMP-7 beads loaded with increased concentrations, presumably due to the chemotactic effect of BMP-7. The highest used concentration of BMP-7 (600µg/ml) dramatically affected the feather patterning.

By increasing the concentration of the inhibitor pulse (Fig. S3 A–C), our model also mimicked previous results obtained by the over-activation of BMP-2 pathway. The area of inhibition, due to the arrest of cell migration, increased with the inhibitor concentration as previously described with BMP-2 (Jung et al., 1998). It also mimicked the results obtained by a global pulse of BMP-2 or BMP-7 over-activation, as described in the RCAS-BMP experiments (Noramly and Morgan, 1998).

Discussion

The expression of BMP target genes such as Id-1, -3 and -4, as shown here, or Msx-1 and Msx-2 previously shown (Chuong et al., 1996) are indicators that the positive effects of the BMP pathway are required for feather morphogenesis. In this study, we propose antagonistic roles for BMP-7 and BMP-2, during feather primordium formation. BMP-7 appeared to act as a chemotactic factor for dermal fibroblasts, this effect of BMP-7 has been described as well on human mesenchymal stem cell (Lee et al., 2006). BMP-2, which is expressed later, appeared to arrest the migration, slowing down cell recruitment to the condensation. The later expression of BMP-4 in the dermal condensation (Noramly and Morgan, 1998) could also act in the arrest of cell migration due to its redundant activity with BMP-2. As previously suggested in the osteogenic differentiation (Hazama et al., 1995), the concomitant presence of BMP-2, BMP-4 and BMP-7 modifies the effect of each factor on cell migration. We propose the BMP pathway as regulator for both the formation of the dermal condensation, and the expression of Id and Msx genes which allowed the continuation of feather morphogenesis.

The different effects of BMP-7 versus BMP-2 and -4 might be linked to the activation of different receptors. Previous studies propose a direct link between cell migration and Activin receptor (ActR) activation in keratinocytes (Zhang et al., 2005). BMP-7 activity is mediated by its fixation on Activin type I and II receptors (ActR-I) (Miyazono, 1999), (ActR-II) (Sebald and Mueller, 2003). These mechanisms involving Rho-GTPases, which are required for fibroblast migration (Michon et al., 2007), they could thus be responsible of dermal cell chemotaxis. By contrast, BMP-2/-4 activity is mediated by their fixation on BMP type I and II receptors (Botchkarev, 2003), and negatively affects cell

migration in at least three manners. First, as BMP-2 in primary cultured dermal fibroblasts regulated the alternative splicing of theEIIIA domain of Fibronectin, we suggest that it might have a similar role in vivo. Indeed, the skin expression pattern of EIIIA reflects the state of dermal organization: formation of dermal condensations (loss of EIIIA expression) and cell proliferation and migration (EIIIA expression). Although there is an increase of Fibronectin deposition in the dermal condensation (Mauger et al., 1982; Michon et al., 2007), EIIIA is spliced out in this area. Second, the loss of EIIIA in dermal condensation correlates, as previously shown in other organs (Manabe et al., 1999; Manabe et al., 1997), with a modification of cell migration and cell proliferation. Indeed, the decrease of EIIIA expression is concomitant with absence of cycling cell in the dermal condensation (Jiang and Chuong, 1992; Wessells, 1965), and could reflect an indirect role for the BMP-2 pathway on cell cycle regulation in the feather primordium. Third, BMP-2 might also regulate the cell migration via a direct effect on Integrin expression. Here we have shown an up-regulation of α4-Integrin expression by BMP-2. Likewise, BMP-2 modulates the expression of β 1-Integrin in osteoblasts (Sotobori et al., 2006), or α2- and α7-Integrin in satellite cells (Ozeki et al., 2007). This direct link between BMP-2 and Integrin expression could explain the rapid effect on primary dermal cells that we observed in our cell migration assay. Thus, the expression of BMP-2 in the dermal condensation microenvironment could explain the arrest of dermal cell migration, through the modulation of adhesion factors.

We propose a new view of BMPs and dermis organization, which is consistent with previous results, although not with their interpretations. It consists out of three major steps; dermal cell migration, follicular domain delimitation, and establishment of follicular domain identity (Fig. 8). Initially there is a limited proliferation along the dorsal midline until a critical cell density is obtained. Then, the molecular dialogue between epidermis and dermis, which leads to primordium formation, can start. Activation of β-catenin in the epidermis (Noramly et al., 1999) is necessary for placode formation and consequently dermal organization. The first permissive dermal signaling is a combination of factors; Wnt, for β-catenin stabilization, and others that initiate FGF-2 and BMP-7 expression in the epidermis (Harris et al., 2004). The loss of either FGF-2, in Scaleless mutant, or BMP-7 function in the epidermis leads to feather defects (Song et al., 1996; Song et al., 2004; Viallet et al., 1998; Harris et al., 2004). Epidermal diffusible chemoattractive factors, BMP-7, as FGF-2 (Song et al., 2004) trigger migration of dermal cells to the placodal area by their chemoattractive effects. Then, the dermal expression of BMP-7, which is regulated by a placodal Wnt signal (Harris et al., 2004), enhances this process. The BMP-2 expression, in placode and then in dermal condensation (Noramly and Morgan, 1998), could modify dermal Integrin expression and regulate splicing of EIIIA, both events leading to a decrease of dermal cell migration capabilities, signifying the second phase of follicular domain delimitation. Two other facts contribute to the limitation of the feather primordium diameter. The induction by BMP-7 of Follistatin expression (Patel et al., 1999) leads to lateral inhibition of BMP signaling, that is reinforced by the expression of Drm/Gremlin in the interfollicular domain (Bardot et al., 2004). Finally, the induction of the Notch system, after BMP-2 expression (Michon, unpublished data), stabilizes (Chen et al., 1997) the follicular domain identity by strengthening its boundaries.

Consistent with these processes, we propose a mathematical model that includes cell proliferation and cell migration by chemotaxis. Our model is still far less intricate than reality. It is a single layer model, which did not take into account the first epidermal BMP-7 impulse, or its role in the stabilization of the formed structures. We also did not take into account a potential heterodimerization between the BMPs. In our model, we have attributed a chemoattractive role to BMP-7 and an arrest role of this chemotaxis to BMP-2. It closely mimics the sequential hexagonal pattern formation observed in vivo and clarified the relation between cell densities and spot formation, which was hinted at in previous in vitro experiments (Jiang et al., 1999). Moreover, we showed that the difference in cell density that is required to switch from the formation of spots to a glabrous area is small (9%). Our mathematical model can also explain our as well as the previous biological results which have concluded that BMP factors act as inhibitors. The use of a point source of high concentration of activator, which induces an over-recruitment of cells, creates an area without the required cell density for dermal condensation formation, and thus mimics the nude area around a BMP-7 coated bead, that was previously interpreted as an inhibitory effect (Patel et al., 1999). Our model explains this result as an over-activation of chemotaxis. Other biological results which were reproduced by our model are the RCAS-BMP-2 skin infection (Noramly and Morgan, 1998), the use of BMP-2 coated beads (Jung et al., 1998), and the addition of BMP-2 in the culture medium (our own experiments). All these methods led to the homogeneous over-activation of BMP-2 in areas which then stay glabrous. Our simulation showed that a local or homogeneous high concentration of the factor that arrests cell migration led to the formation of a glabrous area. Our simulations were specific for BMP over-activation. Although, our model can partially explain the effects of FGF-4 coated beads on chick skin, i.e. the appareance of the typical small inhibition ring around the bead (chemotaxis), it cannot explain the feather bud fusions caused by transformation of interbud region in bud region (Jung et al., 1998; Widelitz et al., 1996).

Our main conclusion is that different members of the BMP family play at least two important roles in chick dermal condensation formation. Firstly, epidermal, then dermal BMP-7 activates the migration of dermal fibroblasts to the appendage domain via chemotaxis; secondly, epidermal, then dermal BMP-2 stops the migration, probably by regulating Integrin and EIIIA expressions. This effect, later reinforced by expression of BMP-4 in the dermis, may lead to the limitation of the dermal condensation size. Moreover, the activation of target

genes such as the Id and Msx families suggests a subtle cell transcriptome regulation in the primordium, due to the transcriptional inhibitor role of Id factors (Kreider et al., 1992; Miyazono and Miyazawa, 2002), and the transcriptional activator role of Msx factors (Lallemand et al, 2005; Ramos and Robert, 2005) during the continuation of feather morphogenesis.

Ackowledgements:

The authors thank Dr. D.J. Pearton and Dr. M. Tummers for critical reading of the manuscript, Dr. N.T. Chattier for the FACS experiments, Mrs B. Peyrusse for the iconography. F. Michon was the recipient of a doctoral fellowship from the French Ministère de la Recherche. This work was supported by the CNRS and by the INSERM.

References:

- Bardot B , Lecoin L , Fliniaux I , Huillard E , Marx M , Viallet JP 2004; Drm/Gremlin, a BMP antagonist, defines the interbud region during feather development. Int J Dev Biol. 48: 149- 56
- Botchkarev VA 2003; Bone morphogenetic proteins and their antagonists in skin and hair follicle biology. J Invest Dermatol. 120: 36- 47
- Chen CW , Jung HS , Jiang TX , Chuong CM 1997; Asymmetric expression of Notch/Delta/Serrate is associated with the anterior-posterior axis of feather buds. Dev Biol. 188: 181- 7
- Chuong CM 1993; The making of a feather: homeoproteins, retinoids and adhesion molecules. Bioessays. 15: 513- 21
- Chuong CM 1998; Molecular Basis of Epithelial Appendage Morphogenesis. Austin.
- Chuong CM , Widelitz RB , Ting-Berreth S , Jiang TX 1996; Early events during avian skin appendage regeneration: dependence on epithelial-mesenchymal interaction and order of molecular reappearance. J Invest Dermatol. 107: 639- 46
- Cruywagen GC , Maini PK , Murray JD 1992; Sequential pattern formation in a model for skin morphogenesis. IMA J math Appl Med Biol. 9: 227- 48
- Desbiens X , Queva C , Jaffredo T , Stehelin D , Vandenbunder B 1991; The relationship between cell proliferation and the transcription of the nuclear oncogenes c-myc, c-myb and c-ets-1 during feather morphogenesis in the chick embryo. Development. 111: 699- 713
- Dhouailly D Editor: Robert L 1977; Dermo-epidermal interactions during morphogenesis of cutaneous appendages in amniotes. In Frontier Matrix Biology. 4: 85- 91
- Dhouailly D Editor: Malacinski G , Bryant S 1984; Specification of feather and scale patterns. Pattern formation. 581- 601 Macmillan Publishing;
- Fliniaux L , Viallet JP , Dhouailly D 2004; Signaling dynamics of feather tract formation from the chick somatopleure. Development. 131: 3955- 66
- Gierer A , Meinhardt H 1972; A theory of biological pattern formation. Kybernetik. 12: 30- 9
- Hamburger V , Hamilton HL 1951; A series of normal stages in the development of the chick embryo. J Morphol. 88: 49- 92
- Harris MP , Linkhart BL , Fallon JF 2004; Bmp7 mediates early signaling events during induction of chick epidermal organs. Dev Dyn. 231: 22- 32
- Hazama M , Aono A , Ueno N , Fujisawa Y 1995; Efficient expression of a heterodimer of bone morphogenetic protein subunits using a baculovirus expression system. Biochem Biophys Res Commun. 209: 859- 66
- Hollnagel A , Oehlmann V , Heymer J , Ruther U , Nordheim A 1999; Id genes are direct targets of bone morphogenetic protein induction in embryonic stem cells. J Biol Chem. 274: 19838- 45
- Houghton L , Lindon C , Morgan BA 2005; The ectodysplasin pathway in feather tract development. Development. 132: 863- 72
- Jaspers M , Wu RR , Van der Schueren B , Cassiman JJ 1995; Localization of alpha 4m integrin at sites of mesenchyme condensation during embryonic mouse development. Differentiation. 59: 79- 86
- Jiang TX , Chuong CM 1992; Mechanism of skin morphogenesis. I. Analyses with antibodies to adhesion molecules tenascin, N-CAM, and integrin. Dev Biol. 150: 82- 98
- Jiang TX , Jung HS , Widelitz RB , Chuong CM 1999; Self-organization of periodic patterns by dissociated feather mesenchymal cells and the regulation of size, number and spacing of primordia. Development. 126: 4997- 5009
- Jiang TX , Widelitz RB , Shen WM , Will P , Wu DY , Lin CM , Jung HS , Chuong CM 2004; Integument pattern formation involves genetic and epigenetic controls: feather arrays simulated by digital hormone models. Int J Dev Biol. 48: 117- 35
- Jung HS , Francis-West PH , Widelitz RB , Jiang TX , Ting-Berreth S , Tickle C , Wolpert L , Chuong CM 1998; Local inhibitory action of BMPs and their relationships with activators in feather formation: implications for periodic patterning. Dev Biol. 196: 11- 23
- Kee Y , Bronner-Fraser M 2001; Id4 expression and its relationship to other Id genes during avian embryonic development. Mech Dev. 109: 341- 5
- Kreider BL , Benezra R , Rovera G , Kadesch T 1992; Inhibition of myeloid differentiation by the helix-loop-helix protein Id. Science. 255: 1700- 2
- Lallemand Y , Nicola MA , Ramos C , Bach A , Cloment CS , Robert B 2005; Analysis of Msx1; Msx2 double mutants reveals multiple roles for Msx genes in limb development. Development. 132: 3003- 14
- Lauffenburger DA 1996; Cell motility. Making connections count. Nature. 383: 390- 1
- Lee DH , Park BJ , Lee MS , Lee JW , Kim JK , Yang HC , Park JC 2006; Chemotactic migration of human mesenchymal stem cells and MC3T3-E1 osteoblast- like cells induced by COS-7 cell line expressing rhBMP-7. Tissue Eng. 12: 1577- 86
- Manabe R , Oh-e N , Sekiguchi K 1999; Alternatively spliced EDA segment regulates fibronectin-dependent cell cycle progression and mitogenic signal transduction. J Biol Chem. 274: 5919- 24
- Manabe R , Ohe N , Maeda T , Fukuda T , Sekiguchi K 1997; Modulation of cell-adhesive activity of fibronectin by the alternatively spliced EDA segment. J Cell Biol. 139: 295- 307
- Mauger A , Demarchez M , Herbage D , Grimaud JA , Druguet M , Hartmann D , Sengel P 1982; Immunofluorescent localization of collagen types I and III, and of fibronectin during feather morphogenesis in the chick embryo. Dev Biol. 94: 93- 105
- Mayerson PL , Fallon JF 1985; The spatial pattern and temporal sequence in which feather germs arise in the white Leghorn chick embryo. Dev Biol. 109: 259- 67
- Michon F , Charveron M , Dhouailly D 2007; Dermal condensation formation in the chick embryo: requirement for integrin engagement and subsequent stabilization by a possible notch/integrin interaction. Dev Dyn. 236: 755- 68
- Miyazono K 1999; Signal transduction by bone morphogenetic protein receptors: functional roles of Smad proteins. Bone. 25: 91- 3
- Miyazono K , Maeda S , Imamura T 2005; BMP receptor signaling: transcriptional targets, regulation of signals, and signaling cross-talk. Cytokine Growth Factor Rev. 16: 251- 63
- Miyazono K , Miyazawa K 2002; Id: a target of BMP signaling. Sci STKE 2002. PE40-
- Noramly S , Freeman A , Morgan BA 1999; beta-catenin signaling can initiate feather bud development. Development. 126: 3509- 21
- Noramly S , Morgan BA 1998; BMPs mediate lateral inhibition at successive stages in feather tract development. Development. 125: 3775- 87
- Norton PA , Hynes RO 1987; Alternative splicing of chicken fibronectin in embryos and in normal and transformed cells. Mol Cell Biol. 7: 4297- 307
- Noveen A , Jiang TX , Ting-Berreth SA , Chuong CM 1995; Homeobox genes Msx-1 and Msx-2 are associated with induction and growth of skin appendages. J Invest Dermatol. 104: 711- 9

- Ogata T , Wozney JM , Benezra R , Noda M 1993; Bone morphogenetic protein 2 transiently enhances expression of a gene, Id (inhibitor of differentiation), encoding a helix-loop-helix molecule in osteoblast-like cells. Proc Natl Acad Sci USA. 90: 9219- 22
- Olivera-Martinez I , Missier S , Fraboulet S , Thelu J , Dhouailly D 2002; Differential regulation of the chick dorsal thoracic dermal progenitors from the medial dermomyotome. Development. 129: 4763- 72
- Olivera-Martinez I , Thelu J , Teillet MA , Dhouailly D 2001; Dorsal dermis development depends on a signal from the dorsal neural tube, which can be substituted by Wnt-1. Mech Dev. 100: 233- 44
- Ozeki N , Jethanandani P , Nakamura H , Ziober BL , Kramer RH 2007; Modulation of satellite cell adhesion and motility following BMP2-induced differentiation to osteoblast lineage. Biochem Biophys Res Commun. 353: 54- 9
- Painter KJ , Maini PK , Othmer HG 1999; Stripe formation in juvenile Pomacanthus explained by a generalized turing mechanism with chemotaxis. Proc Natl Acad Sci USA. 96: 5549- 54
- Patel K , Makarenkova H , Jung HS 1999; The role of long range, local and direct signalling molecules during chick feather bud development involving the BMPs, follistatin and the Eph receptor tyrosine kinase Eph-A4. Mech Dev. 86: 51- 62
- Pummila M , Fliniaux I , Jaatinen R , James MJ , Laurikkala J , Schneider P , Thesleff I , Mikkola ML 2007; Ectodysplasin has a dual role in ectodermal organogenesis: inhibition of Bmp activity and induction of Shh expression. Development. 134: 117- 25
- Ramos C , Robert B 2005; msh/Msx gene family in neural development. Trends Genet. 21: 624- 32
- Rouzankina I , Abate-Shen C , Niswander L 2004; Dlx genes integrate positive and negative signals during feather bud development. Dev Biol. 265: 219- 33
- Scaal M , Prols F , Fuchtbauer EM , Patel K , Hornik C , Kohler T , Christ B , Brand-Saberi B 2002; BMPs induce dermal markers and ectopic feather tracts. Mech Dev. 110: 51- 60
- Sebald W , Mueller TD 2003; The interaction of BMP-7 and ActRII implicates a new mode of receptor assembly. Trends Biochem Sci. 28: 518- 21
- Sengel P 1976; Morphogenesis of Skin. Cambridge
- Song H , Wang Y , Goetinck PF 1996; Fibroblast growth factor 2 can replace ectodermal signaling for feather development. Proc Natl Acad Sci USA. 93: 10246- 9
- Song HK , Lee SH , Goetinck PF 2004; FGF-2 signaling is sufficient to induce dermal condensations during feather development. Dev Dyn. 231: 741- 9
- Sotobori T , Ueda T , Myoui A , Yoshioka K , Nakasaki M , Yoshikawa H , Itoh K 2006; Bone morphogenetic protein-2 promotes the haptotactic migration of murine osteoblastic and osteosarcoma cells by enhancing incorporation of integrin beta 1 into lipid rafts. Exp Cell Res. 312: 3927- 38
- Tao H , Yoshimoto Y , Yoshioka H , Nohno T , Noji S , Ohuchi H 2002; FGF10 is a mesenchymally derived stimulator for epidermal development in the chick embryonic skin. Mech Dev. 116: 39- 49
- Turing AM 1952; The chemical basis of morphogenesis. Phil Trans R Soc Lond II. 37- 72
- Viallet JP , Prin F , Olivera-Martinez I , Hirsinger E , Pourquie O , Dhouailly D 1998; Chick Delta-1 gene expression and the formation of the feather primordia. Mech Dev. 72: 159 - 68
- Wessells NK 1965; Morphology and proliferation during early feather development. Dev Biol. 12: 131- 53
- Widelitz RB , Jiang TX , Noveen A , Chen CW , Chuong CM 1996; FGF induces new feather buds from developing avian skin. J Invest Dermatol. 107: 797- 803
- Wilkinson DG , Nieto MA 1993; Detection of messenger RNA by in situ hybridization to tissue sections and whole mounts. Methods Enzymol. 225: 361- 73
- Zhang L , Deng M , Parthasarathy R , Wang L , Mongan M , Molkentin JD , Zheng Y , Xia Y 2005; MEKK1 transduces activin signals in keratinocytes to induce actin stress fiber formation and migration. Mol Cell Biol. 25: 60- 5

Figure 1

Some BMP pathway factor expressions during feather primordium formation(A–D)

The left and right femoral tract of the same HH30 embryo were compared, the numbers correspond to the order of appearance of rows. The second row (R2) had only two feather primordia expressing BMP-2 (**A**), whereas five expressed BMP-7 (**B**). The additional primordia are noted with red and corresponding ones with black arrows. The distal border (yellow arrow), which preceded the appearance of R3, delimited the femoral and zeugopodial tracts and already expressed BMP-7 (**B**) but not BMP-2 (**A**). In another embryo, R4 was expressing BMP-2 on the left side (**C**) while Follistatin was expressed only in three rows on the right (**D**). A continuous line, contiguous to R3, was the distal border of the tract, which expressed Follistatin and not BMP-2. (**E–G**) Ids expression in the dorsal tract of HH30 embryos. There was a decrease of ld-l expression from the new formed (black arrow) to the older ones (red arrow) (**E**). Id-3 transcripts showed a stable expression in the primordia (**F**). Id-4 expression exhibited an early expression on the entire primordia (black arrow), and a later expression restricted to a peripheral ring (red arrow) (**G**). In situ hybridization with RNA probes. Bars: **A–D**: l000µm. Bars: **E–G**: 800µm.

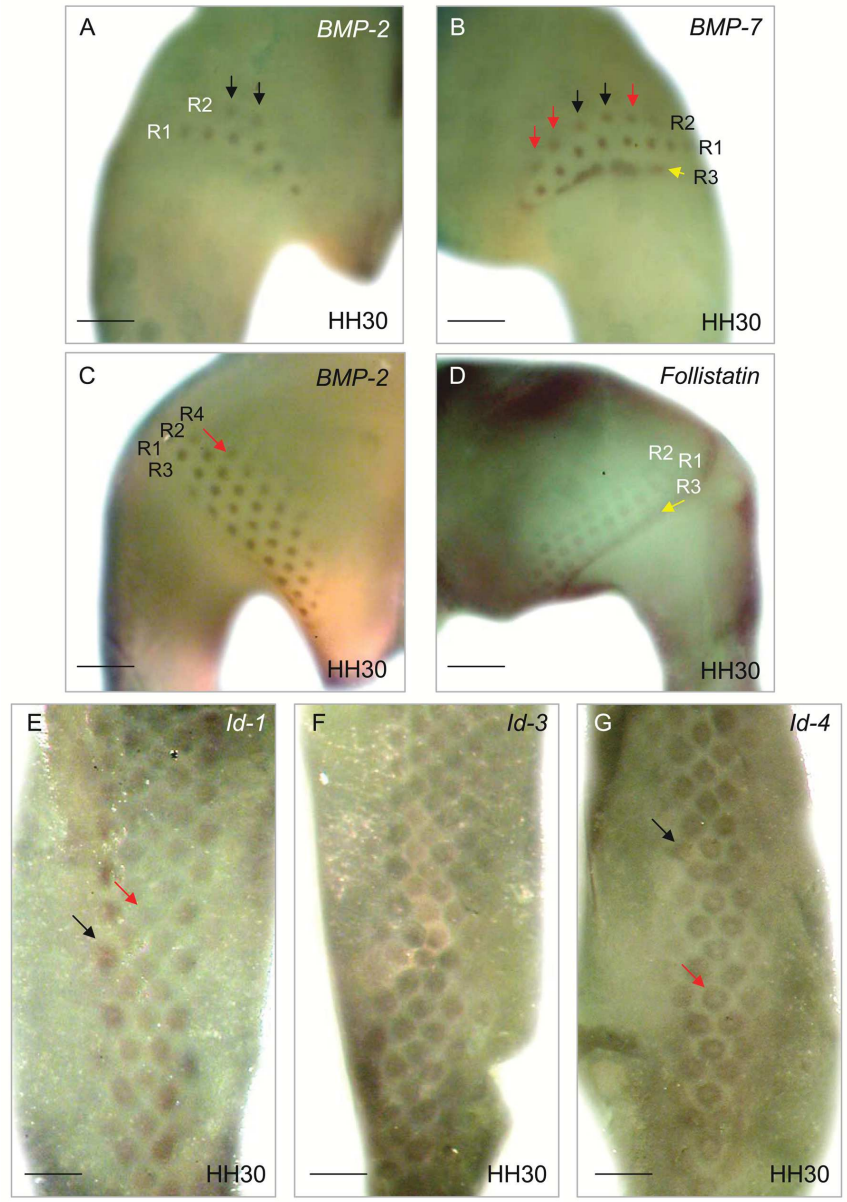

Figure 2

Comparative effects of BMP-2 and BMP-7 on dermal fibroblasts cytokinesis

A freshly dissociated dermal cell suspension was added to a cell culture insert and basic medium placed on the other side of the 8µm pore membrane. Two types of controls were performed: two of basic media (+/− FBS), and two with or without FGF-2. The first control allowed a normalization of the cell migration measurement (50.1% and 100%); the second, the validation of the chemotaxic effect with FGF-2 (60.8% and 110.9%). BMP-7 had an even stronger chemotactic effect (70.1% and 122.3%). Perturbation of fibroblast migration was clearly shown with BMP-2 (38.1% and 81.6%). The chemotaxis obtained with BMP-7 decreased with the addition of BMP-2 (51.2% and 98.2%). The migration was evaluated in triplicate by a fluorescent method. The Student's t-test has a relevance of $p<0.05$. BMP-2 and BMP-7: 0.5µg/ml; FGF-2: 0.33µg/ml.

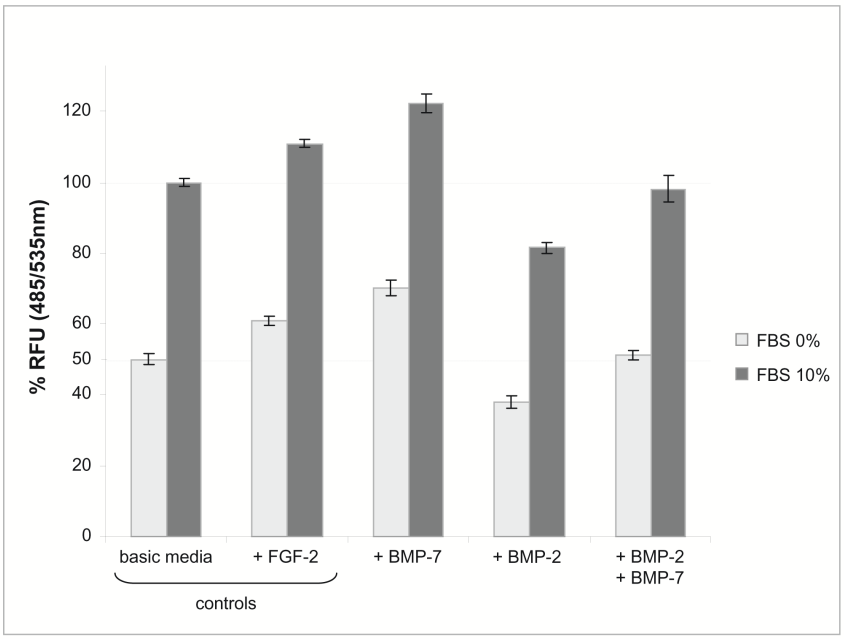

Figure 3

The Fibronectin exon EniA was involved in dermal organization

(A–B) Chick embryo dorsal skin. At HH29+, EIIIA was expressed in the periphery (red arrow) of the first feather primordia, as well as in two ribbons on either side of the first row (black arrows) (**A**). At HH30, the EIIIA transcripts were expressed in the periphery of primordia and in two ribbons (black arrows) on either side of feather rows, while there was a slightly decrease of its expression in the three first rows (red arrow) (**B**). (**C–D**) BMP-2 and EIIIA expressions in the left and right femoral tract of the same HH30 embryo. Five feather primordia of the fourth row (R4) expressed BMP-2 (**C**), while only two in the corresponding right row (**D**). The additional primordia were noted with red arrows and corresponding ones with black arrows. The R3, expressing the EIIIA has started to form close to the distal border line.

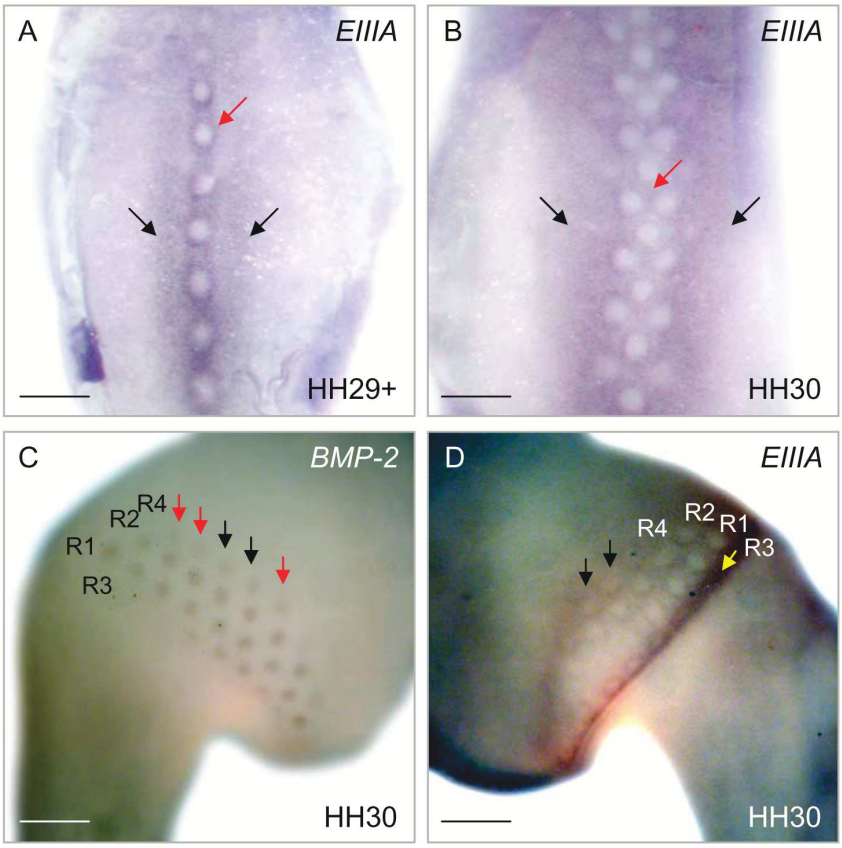

Figure 4

The regulation of EIIIA and (α4-Integrin expressions

(A–B) EIIIA expression in cultured dermal fibroblasts in hanging drops for 24, 48 or 72 hours. RT-PCR for Actin, total Fibronectin and EIIIA exon were performed. The Fibronectin expression was normalized with Actin expression. There is a small decrease in Fibronectin expression between t_0 (100%) and t_{48} (92.8%), and, a significant decrease at t_{72} (64.1%) (**A**). The EIIIA expression was normalized to Fibronectin expression. During the same time laps, the portion of Fibronectin containing the EIIIA exon decreased from 59.4% to 24.3% (**B**). (**C–D**) Cells were placed in adherent culture with or without BMP-2 and BMP-7 for 20 hours and RT-PCR to detect EIIIA and Integrin-α4 expressions were performed. The part of Fibronectin containing EIIIA decreased with BMP-2 treatment, from 61.1% to 34.4%, whereas the BMP-7 treatment led to a non significant decrease, 53.1% (**C**). The BMP-2 treatment led to an increase of α4-Integrin expression, from 100% to 125.29% whereas BMP-7 induced only a non significant increase (105.5 %) (**D**). BMP-2, BMP-7: 0.5µg/ml.

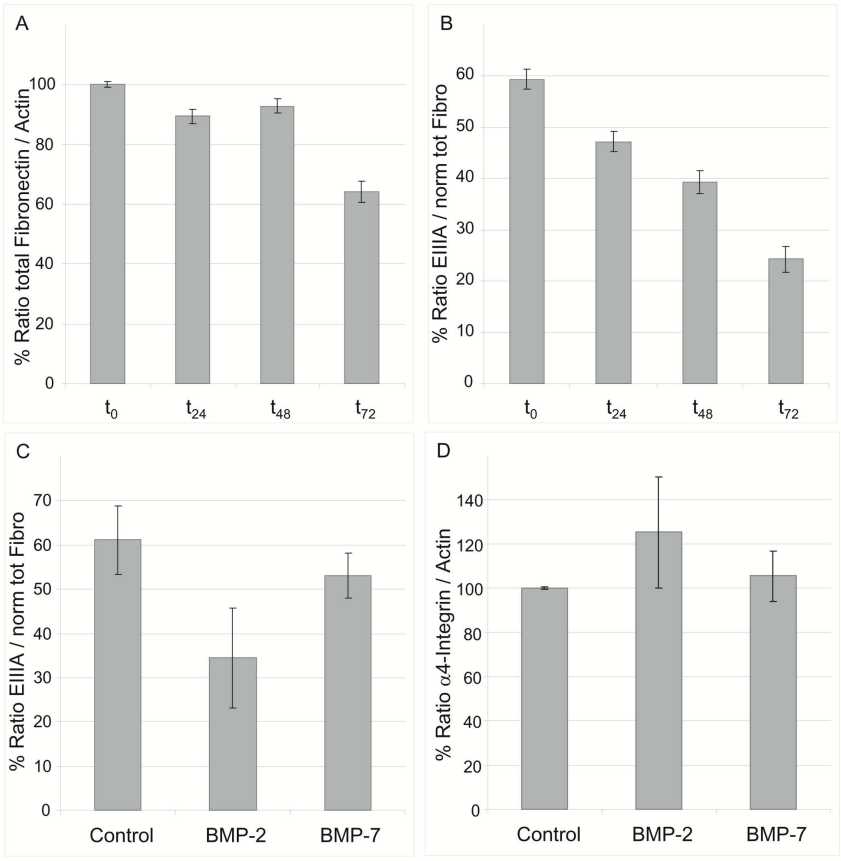

Figure 5

Sequential appearance and patterning of spots with mathematical simulation

The resolution of the model led to the formation of a primary migrating cell midline (**A**). The redistribution of these cells, via chemotaxis, led to the formation of spots, while laterally new cells started to migrate (**B**). The lateral expansion of the pattern was due to migrating cells under both chemotactic and arresting factors (**C**). At the end of the simulation, the hexagonal pattern occurred all over the modeled domain (**D**). Cell density is represented in false colors.

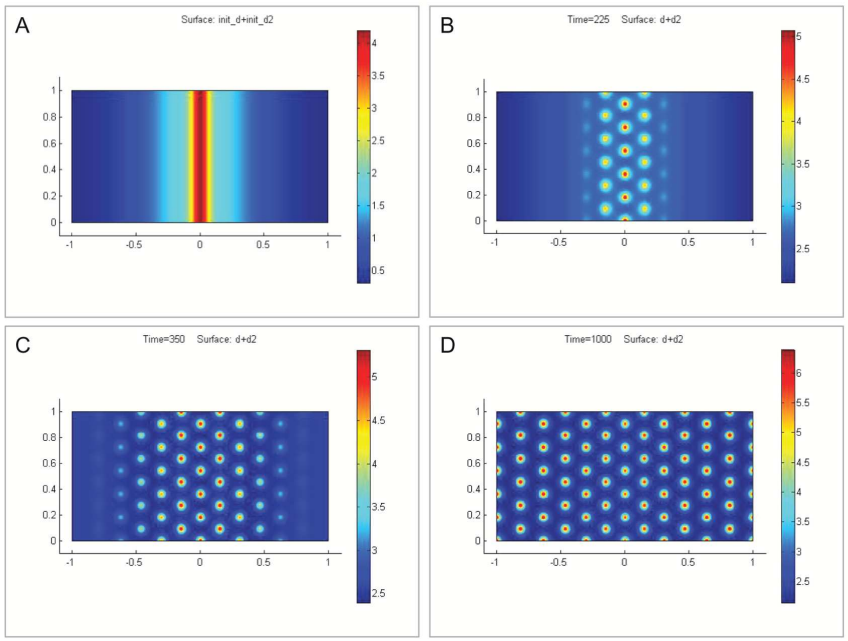

Figure 6

The progressive increase of the cell density correlated successively with the formation of an apterium, a semi-apterium and a pteryla

The pteryla was characterized by a regular pattern (**A**). The decrease of cell density (q) to 0.2 (**B**) and 0.12 (**C**) led respectively to an irregular pattern as at the boundary of a pteryla and a semi-apteria. The switch from spot formation to a glabrous region (**D**) implicated only a small difference in cell density (q=0.12 versus q=0.11).

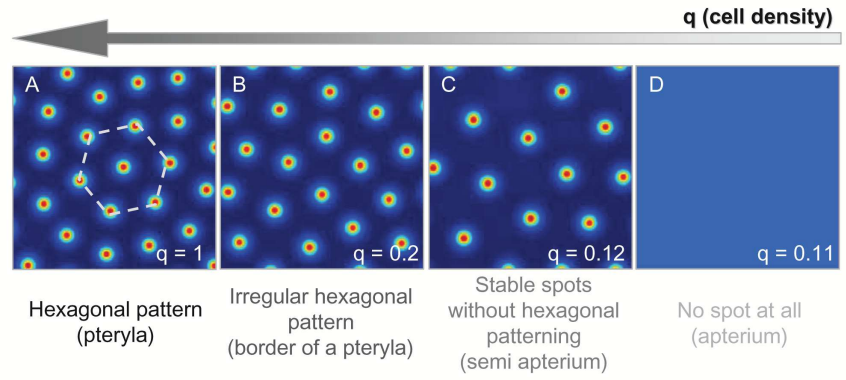

Figure 7

Over-activation of chemoattraction led to similar results with mathematical simulation and organotypic culture

(A–C). Simulation of a local pulse of activator led to the formation of an accumulation of cells, surrounded with a ring of inhibition. The size of this ring was proportional to the activator concentration. (D–F) Patterns resulted from a local application of BMP-7 coated beads. The maximal area of inhibition (red circle) was obtained with the maximal concentration of BMP-7. pu(x,y)=c*exp(−(x^2+(y−0.5)^2)*500) with c=4 ; 8 or 24 Bars: 250µm.

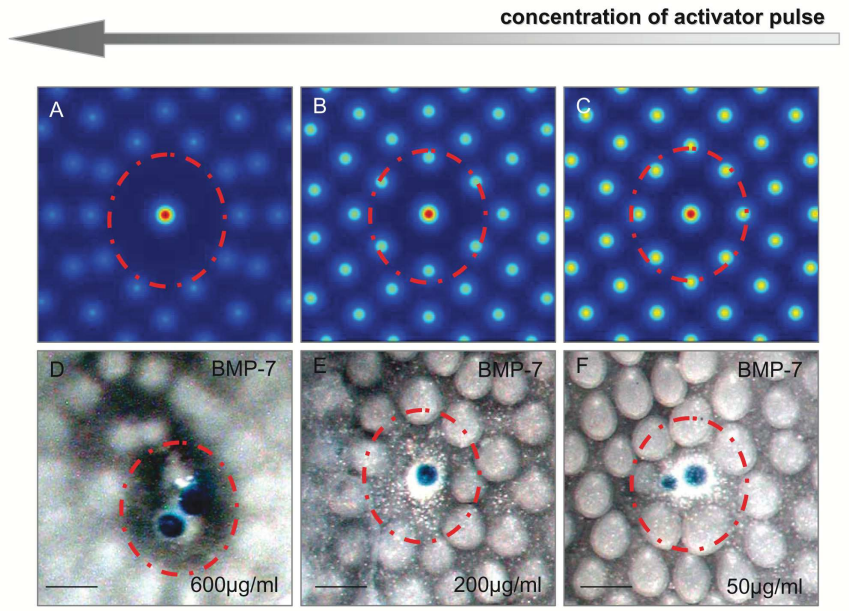

Figure 8

Model of dermal condensation formation in dorsal chick embryo skin

The chronological events from dense dermis to stabilized dermal condensation require a molecular dialogue inter- and intra- tissular in the skin (see the text). Note that the placodes are larger and earlier than the dermal condensations (Dhouailly, 1984). This model only took into account the BMPs as well as a few other important genes among those expressed in embryonic skin.